HHS Public Access

Author manuscript

Biol Psychiatry. Author manuscript; available in PMC 2018 July 01.

Published in final edited form as:

Biol Psychiatry. 2017 July 01; 82(1): 40–48. doi:10.1016/j.biopsych.2016.09.018.

Alterations in a unique class of cortical chandelier cell axon cartridges in schizophrenia

Brad R. Rocco, Ph.D.[1], **Adam M. DeDionisio, B.S.**[1], **David A. Lewis, M.D.**[1,2], and **Kenneth N. Fish, Ph.D.**[1]

[1]Department of Psychiatry, University of Pittsburgh School of Medicine, Pittsburgh, PA 15213

[2]Department Neuroscience, University of Pittsburgh School of Medicine, Pittsburgh, PA 15213

Abstract

Background—The axons of chandelier cells (ChCs) target the axon initial segment (AIS) of pyramidal neurons, forming an array of boutons termed a cartridge. In schizophrenia, the density of cartridges detectable by GABA membrane transporter-1 (GAT1) immunoreactivity is lower, whereas the density of AISs detectable by immunoreactivity for the α2 subunit of the GABA-A receptor is higher in layers 2-superficial 3 of the prefrontal cortex (PFC). These findings were interpreted as compensatory responses to lower GABA levels in ChCs. However, we recently found that in schizophrenia ChC cartridge boutons contain normal levels of the 67 kDa isoform of glutamic acid decarboxylase (GAD67) protein, the enzyme responsible for GABA synthesis in these boutons. To understand these findings we quantified the densities of ChC cartridges immunoreactive for vesicular GABA transporter (vGAT+), which is present in all cartridge boutons, and the subset of cartridges that contain calbindin (CB+).

Methods—PFC tissue sections from 20 matched pairs of schizophrenia and unaffected comparison subjects were immunolabeled for vGAT, GAD67, and CB.

Results—The mean density of vGAT+/CB+ cartridges was 2.7-fold higher, exclusively in layer 2 of schizophrenia subjects, whereas the density of vGAT+/CB− cartridges did not differ between subject groups. Neither vGAT, CB, or GAD67 protein levels per ChC bouton, nor the number of boutons per cartridge, differed between subject groups.

Conclusions—Our findings of a greater density of CB+ ChC cartridges in PFC layer 2 from schizophrenia subjects suggests that the normal developmental pruning of these cartridges is blunted in the illness.

Correspondence should be addressed to: Dr. Kenneth N. Fish, Ph.D., Department of Psychiatry, Western Psychiatric Institute and Clinic, University of Pittsburgh, Biomedical Science Tower, Room W1651, Tel: 412-648-9366; Fax: 412-624-9910, fishkn@upmc.edu.

Financial Disclosures

Dr. Rocco, Mr. DeDionisio, and Dr. Fish report no biomedical financial interests or potential conflicts of interest.

Keywords

GAD67; vGAT; gamma-aminobutyric acid; quantitative microscopy; axo-

Introduction

Cognitive impairments are a core feature of schizophrenia and the best predictor of functional outcome (1). Cognitive deficits in schizophrenia are associated with dysfunction of the prefrontal cortex (PFC), which is thought to reflect, at least in part, alterations in cortical γ-aminobutyric acid (GABA) neurons. For example, multiple studies have found lower mRNA levels of the 67 kDa isoform of the GABA synthesizing enzyme glutamic acid decarboxylase (GAD67) in the PFC of subjects with schizophrenia (2–12). At the cellular level, two groups found that GAD67 mRNA levels were markedly lower in ~25–35% of neurons across PFC layers 2-superficial 3 (2, 12) although no difference was observed in a third study (13). Importantly, neither the total number of neurons (2, 14), nor the number of GABA neurons (13), appears to be altered in the PFC of subjects with schizophrenia. In concert, these findings suggest that a subset of GABA neurons exhibit very low levels of GAD67 expression in schizophrenia. In support of this interpretation, GAD67 protein levels were found to be markedly lower in a subset of axonal boutons identified by immunoreactivity for the vesicular GABA transporter (vGAT) (15), which is responsible for packaging GABA into ready-releasable synaptic vesicles.

Other lines of evidence suggest that the affected GABA neurons might include the chandelier (axo-axonic) cell (ChC). The axons of ChCs exclusively target the axon initial segment (AIS) of pyramidal neurons. The axon of a given ChC diverges to innervate hundreds of neighboring pyramidal neurons, and the axons of multiple ChCs may converge onto a single pyramidal neuron AIS, forming a distinctive, vertically-oriented array of boutons termed a cartridge (16). In schizophrenia, the density of cartridges detected by immunoreactivity for the GABA membrane transporter-1 (GAT1+), a protein responsible for preventing spillover and for reuptake of released GABA into the synaptic bouton, is lower, with the greatest deficit in PFC layers 2-superficial 3 (17, 18). In these same layers, the density of AISs detectable by immunoreactivity for the α2 subunit of the GABA-A receptor is increased by >100% in schizophrenia compared to unaffected comparison subjects (19). These pre- and postsynaptic changes in GAT1 and GABA-A α2 subunit immunoreactivity are inversely correlated (19), and were interpreted as reciprocal compensatory responses due to lower GAD67 expression, and presumably less GABA available for release, from ChC boutons (20). However, this interpretation is challenged by our recent report that GAD67 protein levels are not altered in vGAT+ ChC cartridge boutons in schizophrenia (15).

The finding of lower GAT1+ cartridge density in schizophrenia was thought to reflect lower GAT1 protein levels in ChC boutons such that some cartridges were no longer detectable with immunohistochemical techniques. However, the methods employed could not exclude the alternative possibility that schizophrenia is associated with an actual reduction in the number of cartridges. To distinguish between these alternatives, we quantified the densities of cartridges immunoreactive for vesicular GABA transporter (vGAT+) since neither vGAT

mRNA expression (21) nor cartridge bouton vGAT protein levels are altered in the PFC of schizophrenia subjects (15). Thus, vGAT+ cartridge density measures directly index the number of cartridges present. In addition, while studying human PFC tissue immunohistochemically labeled for the calcium-binding protein calbindin (CB) in a separate study, we observed a high density of CB+ cartridges, which were previously reported in human temporal cortex (22). Since the prior findings of GAT1+ ChC cartridge alterations were most marked in layers 2-superficial 3, we also examined the subset of cartridges that contain CB in those layers.

Methods and Materials

Subjects

Brain specimens from 40 subjects were recovered during autopsies conducted at the Allegheny County Medical Examiner's Office (Pittsburgh, PA, USA) after obtaining consent from the next of kin. An independent committee of experienced research clinicians made consensus DSM-IV diagnoses, or confirmed the absence of any diagnoses, for each subject using the results of structured interviews conducted with family members and/or review of medical records (7). To reduce biological variance between groups, and to employ a design that controlled for experimental variance, each schizophrenia subject was matched to one unaffected comparison subject for sex, and as closely as possible for age and postmortem interval (PMI) (Table 1 and Supplemental Table S1). The length of the PMI can affect protein integrity (23, 24) and aging can differentially affect gene expression (25). Consequently, to reduce the potential effects of these confounding variables we selected all available subjects with PMI < 16 hours and age ≤ 55 years. Mean age, PMI and tissue storage time did not differ between subject groups (Table 1). The University of Pittsburgh's Committee for the Oversight of Research and Clinical Trials Involving the Dead and Institutional Review Board for Biomedical Research approved all procedures.

The left hemisphere of each brain was blocked coronally at 1–2 cm intervals, immersed in 4% paraformaldehyde for 48 hours at 4°C and then washed in a series of graded sucrose solutions and cryoprotected. Tissue blocks containing the PFC were sectioned coronally at 40 μm on a cryostat and stored in a 30% glycerol/ 30% ethylene glycol solution at −30° C until processed for immunohistochemistry.

Immunohistochemistry

For each subject, four sections containing PFC area 9, identified from nearby Nissl-stained sections, and spaced ~500 μm apart were used (80 sections total). To minimize experimental variance within and across subject pairs, two experimental runs were performed in which two sections per subject were processed simultaneously. The sodium citrate antigen retrieval method (26) was performed to enhance immunostaining followed by section permeabilization with 0.3% Triton X-100 in PBS for 30 minutes at room temperature (RT). Sections were then blocked using 20% donkey serum in PBS for 2 hours at RT, and incubated for ~72 hours at 4°C in PBS containing 2% donkey serum and primary antibodies. The antibodies for both runs were the same except that one run included an antibody directed against CB. The antibodies used recognized vGAT (mouse host; 1:500, Synaptic

Systems, Goettingen, Germany; product # 131011, Lots 131011/41 and 131011/42), GAD67 (goat host; 1:100, R&D Systems, Minneapolis, MN, USA; product # AF2086, Lot KRD0110031), and CB (rabbit host; 1:1000; Swant, Switzerland; product # CB-38a, Lot 9.03). The specificity of each antibody was verified in our laboratory (27, 28) or other laboratories (vGAT (29); GAD67 (30, 31)). In addition, the specificity of each antibody was assessed in preabsorption experiments (Supp. Fig. S1). Sections were then rinsed for 2 hours in PBS and incubated for 24 hours in PBS containing 2% donkey serum and secondary antibodies (donkey host) conjugated to biotin (1:250; CB), Alexa 488 (1:500; vGAT), or Alexa 647 (1:500; Invitrogen, Grand Island, NY, USA for all; GAD67) at 4°C. Next, the sections were rinsed in PBS (2 hours), incubated with streptavidin Alexa 405 (1:200; CB) for 24 hours, rinsed in PBS (2 hours), mounted (ProLong Gold antifade reagent, Invitrogen) on slides, which were coded to conceal diagnosis and subject number, and then stored at 4°C until imaged. Secondary antibody specificity was verified by omitting the primary antibody in control experiments Supp. Fig. S1). Multiple pilot studies were performed to determine if any primary/secondary combinations influenced the outcome; results from these studies indicated that the ability to detect each antigen was not dependent on the secondary antibody spectra.

Microscopy

Data were collected on an Olympus (Center Valley, PA) IX81 inverted microscope equipped with an Olympus spinning disk confocal unit, Hamamatsu EM-CCD digital camera (Bridgewater, NJ), and high precision BioPrecision2 XYZ motorized stage with linear XYZ encoders (Ludl Electronic Products Ltd., Hawthorne NJ) using a 60× 1.40 N.A. SC oil immersion objective. The equipment was controlled by SlideBook 5.0 (Intelligent Imaging Innovations, Inc., Denver, CO), which was the same software used for post-image processing. 3D image stacks (2D images successively captured at intervals separated by 0.25 μm in the z-dimension) that were 512 × 512 pixels (~ 137 × 137 μm) were acquired over 50 percent of the total thickness of the tissue section starting at the coverslip. Importantly, imaging the same percentage, rather than the same number of microns, of the tissue section thickness controls for the potential confound of storage and/or mounting related volume differences (i.e. z-axis shrinkage). The stacks were collected using optimal exposure settings (i.e., those that yielded the greatest dynamic range with no saturated pixels), with differences in exposures normalized during image processing.

Sampling

As determined by measurements made in Nissl-stained sections (18), the boundaries of the six cortical layers can be estimated based on the distance from the pial surface to the white matter: 1 (pia-10%), 2 (10–20%), 3 (20–50%), 4 (50–60%), 5 (60–80%), and 6 (80%-gray/white matter border). Ten systematic randomly sampled image stacks per section were taken within each layer using a sampling grid of 180 × 180 μm^2. The same investigator (BRR), who was blind to subject and diagnosis, collected all image stacks. Sections within a run from both subjects in a pair were imaged on the same day. Note that the initial analysis was conducted in layers 2-superficial 3 (i.e., 10–35% of the distance from the pial surface to the layer 6 white matter border).

Image processing

Each fluorescent channel was deconvolved using Autoquant's Blind Deconvolution algorithm. Data segmentation was performed as described (32). Lipofuscin autofluorescence, a potential confound of quantitative fluorescence measures in human cortex, was excluded as described in Supplemental Methods. In all sections, vGAT+ punctate structures, presumed GABA axon boutons (33, 34), were distributed across all cortical layers of the PFC, with the greatest intensity of labeling in the superficial layers. Amid this general punctate labeling, distinct parallel arrays of immunoreactive axonal boutons were readily identified (Fig. 1 and Supp. Fig. S2). These structures are morphologically identical to the vGAT+ cartridges that have previously been shown to represent ChC boutons innervating the AIS of pyramidal neurons (35). In addition, in human PFC vGAT is present in ChC cartridge boutons at twice the average level of other GABA boutons, making vGAT+ cartridges easily identifiable amid the general punctate vGAT labeling in gray matter (15). Furthermore, levels of vGAT protein in cartridge boutons are unaltered in the PFC of schizophrenia subjects (15). Thus, vGAT immunoreactivity is an ideal marker of ChC cartridges because counting vGAT+ cartridges will not be confounded by disease-associated differences in ChC bouton vGAT protein levels. Within each image stack, an unbiased counting frame (~68×68 μm^2), consisting of two exclusion lines and two inclusion lines, was used to identify vGAT+ cartridges for analysis. vGAT+ cartridges were included for analysis and manually traced only if they were considered to be completely visualized as indicated by 1) continuity across z planes and 2) the presence of the entire cartridge within a virtual sampling box. The virtual sampling box started and ended one z-plane from the top and bottom of the image stack, respectively, and had x-y start/end coordinates that were located 20 pixels from any edge. The presence of an unlabeled soma and the tapered ending of continuous vGAT labeling determined the beginning and end of the cartridge, respectively. Figure 1E shows a traced vGAT+ cartridge. For a cartridge to be classified as being CB+ it needed to be identifiable by CB immunoreactivity independent of vGAT immunoreactivity. Importantly, a single investigator (AMD) blind to diagnosis and layer assessed all image stacks in a randomized order for the presence of cartridges.

Statistics

Two analyses of covariance (ANCOVA) models were used to compare group differences. Because subjects were selected and processed as pairs, the first paired ANCOVA model included cartridge density, bouton number or fluorescence intensity (relative protein) level as the dependent variable, diagnostic group as the main effect, subject pair as a blocking factor, and tissue storage time as a covariate. Subject pairing is an attempt to balance diagnostic groups for sex, age, and PMI, and to account for the parallel processing of tissue samples, and thus is not a true statistical paired design. Consequently, a second unpaired ANCOVA model was performed that included all covariates (i.e., age, sex, PMI, storage time). All statistical tests were conducted with α-level= 0.05.

We also assessed the potential influence of other factors that are frequently comorbid with the diagnosis of schizophrenia using ANCOVA models. For these analyses, we conducted comparisons among groups of subjects with schizophrenia, using each grouping variable (sex; diagnosis of schizoaffective disorder; nicotine use at the time of death; use of

antipsychotics, antidepressants, or benzodiazepines and/or sodium valproate at the time of death) as the main effect and age, tissue storage time, and PMI as covariates. A Bonferroni-adjusted α-level of 0.05/6 = 0.008 was used to assess significance.

Reported ANCOVA statistics include only those covariates that were statistically significant. As a result, the reported degrees of freedom vary across analyses.

Results

The initial analysis was performed in layers 2-superficial 3 of the PFC because in schizophrenia the greatest deficits of GAT1+ cartridge density were found in these layers (17, 18). Within layers 2-superficial 3, the density of vGAT+ cartridges was 21% higher (paired, $F_{1, 19} = 4.65$, $p = 0.044$; unpaired, $F_{1, 38} = 5.01$, $p = 0.031$) in schizophrenia (16,598 ± 3,993 cartridges/mm^3) relative to unaffected comparison (13,747 ± 4,069 cartridges/mm^3) subjects (Fig. 2A). Both the amount of protein per bouton and the number of boutons per cartridge can influence cartridge detectability. Importantly, vGAT protein levels in cartridge boutons did not differ (paired, $F_{1, 18} = 1.36$, $p = 0.258$; unpaired, $F_{1, 37} = 0.75$, $p = 0.392$) between schizophrenia (1,370 ± 252 a.u.) and comparison (1,316 ± 236 a.u.) subjects (Fig. 2B). In addition, the mean number of vGAT+ boutons per cartridge did not differ (paired, $F_{1, 19} = 0.0$, $p = 0.994$; unpaired, $F_{1, 37} = 0.0$, $p = 0.995$) between schizophrenia (17.98 ± 2.11 boutons/cartridge) and comparison (17.98 ± 2.61 boutons/cartridge) subjects (Fig. 2C–D). In concert, these findings indicate that the greater density of vGAT+ cartridges in schizophrenia is not attributable to a greater detectability of a normal complement of ChC-to-pyramidal neuron AIS inputs.

While studying human PFC tissue immunohistochemically labeled for CB, we observed the presence of CB+ cartridges in cortical layers 2–6. A quantitative analysis of CB+ cartridge number performed here in unaffected comparison subjects found that 15% of vGAT+ cartridges in PFC layers 2-superficial 3 contained CB protein (Fig. 3). Therefore, the density of vGAT+/CB+ cartridges within PFC layers 2-superficial 3 was assessed to determine if the vGAT+ cartridge density finding was driven by changes in a subset of ChC cartridges. The density of vGAT+/CB+ cartridges within PFC layers 2-superficial 3 was 141.1% higher (paired, $F_{1, 19} = 9.58$, $p = 0.006$; unpaired, $F_{1, 38} = 9.39$, $p = 0.004$) in schizophrenia (3,912 ± 2,570 cartridges/mm^3) relative to unaffected comparison (1,623 ± 2,135 cartridges/mm^3) subjects (Fig. 4A). In contrast, the density of vGAT+/CB− cartridges did not differ (paired, $F_{1, 19} = 0.011$, $p = 0.917$; unpaired, $F_{1, 38} = 0.012$, $p = 0.913$) between schizophrenia (7,636 ± 2,895 cartridges/mm^3) and unaffected comparison (7,544 ± 2,345 cartridges/mm^3) subjects (Fig. 4B). A laminar analysis of vGAT+/CB+ and vGAT+/CB− cartridge densities found that the increase in vGAT+/CB+ cartridge density was confined to layer 2 and specific for vGAT+/CB+ cartridges (Fig. 4C–D and Fig. 5A). Specifically, within layer 2 the density of vGAT+/CB+ cartridges was 2.7-fold (173.5%) higher (paired $F_{1, 19} = 11.83$, $p = 0.003$; unpaired $F_{1, 38} = 13.55$, $p = 0.001$) in schizophrenia (5,907 ± 3,431 cartridges/mm^3) relative to unaffected comparison (2,160 ± 2,992 cartridges/mm^3) subjects (Fig. 5A). A qualitative assessment of the individual subject data suggested that one control and two schizophrenia subjects might be outliers. Thus, the ‘outlier labeling rule’ (36, 37) was used to assess the vGAT+/CB+ cartridge density data. The three aforementioned subjects were identified as

outliers. Therefore, an additional analysis was performed after removing the affected subject pairs. In this analysis, the density of vGAT+/CB+ cartridges was 2.9-fold (193.6%) higher (paired $F_{1, 16} = 18.43$, $p = 0.001$; unpaired $F_{1, 32} = 20.99$, $p < 0.0005$) in schizophrenia (5,041 ± 2,292 cartridges/mm^3) relative to unaffected comparison (1,717 ± 1,921 cartridges/mm^3) subjects. In contrast, neither vGAT+/CB+ nor vGAT+/CB− cartridge density were altered in schizophrenia in cortical layers 3, 4, 5, or 6 (Fig. 4C–D). Within vGAT+/CB+ cartridge boutons in layer 2, protein levels did not differ between subject groups for CB (paired $F_{1, 11} = 0.013$, $p = 0.910$; unpaired $F_{1, 31} = 0.327$, $p = 0.572$; Fig. 5B), vGAT (paired $F_{1, 12} = 1.369$, $p = 0.265$; unpaired $F_{1, 31} = 0.988$, $p = 0.328$; Fig. 5C), or GAD67 (paired $F_{1, 12} = 0.087$, $p = 0.772$; unpaired $F_{1, 31} = 0.045$, $p = 0.834$; Fig. 5D).

The higher density of layer 2 vGAT+ cartridges in schizophrenia did not appear to be due to comorbid factors that frequently accompany the illness. Specifically, within schizophrenia subjects, vGAT+/CB+ cartridge density did not differ as a function of sex, nicotine use at time of death (ATOD), benzodiazepines and/or sodium valproate ATOD, antidepressants ATOD, antipsychotics ATOD, or diagnosis of schizoaffective disorder (Fig. 6). In addition, vGAT+/CB+ cartridge density did not differ as a function of duration of illness ($F_{1, 18} = 0.893$, $p = 0.606$), suggesting that our findings are not a consequence of factors associated with illness chronicity.

Discussion

Prior studies found that the density of GAT1+ cartridges was lower in the PFC of schizophrenia subjects, particularly in layers 2-superficial 3 (17, 18). GAT1 in the presynaptic bouton membrane regulates the levels and diffusion of extracellular GABA via re-uptake. Thus, it was suggested that ChC bouton GAT1 protein levels were lower in schizophrenia to compensate for lower GABA levels in ChC boutons, resulting in fewer cartridges being detectable by GAT1 immunoreactivity. However, it was recently reported that ChC bouton GAD67 and vGAT protein levels are unchanged in schizophrenia (15), leading us to suggest an alternative explanation for the GAT1+ cartridge findings: fewer cartridges are present in the illness. Surprisingly, the findings of the present study reveal that schizophrenia is associated with a 2.7-fold higher density of vGAT+/CB+ cartridges in layer 2 relative to unaffected comparison subjects. These findings were layer- and cell type-specific because vGAT+/CB− cartridge density is unchanged in layer 2, and neither vGAT +/CB+ nor vGAT+/CB− cartridge density is altered across layers 3–6.

The detectability of a cartridge is dependent on the expression levels of the proteins used to visualize them. Thus, the proportion of vGAT+ cartridges classified as CB+ would presumably increase in the presence of elevated levels of CB in ChC boutons. However, CB protein levels did not differ between subject groups within vGAT+/CB+ cartridge boutons in layer 2. In addition, vGAT+/CB− cartridge density was not altered in schizophrenia, suggesting that in the disease CB protein levels are not elevated in a subset of cartridges normally classified as being CB−. The number of boutons per cartridge can also influence cartridge detectability, but the mean number of vGAT+ boutons per cartridge did not differ between schizophrenia and comparison subjects. In concert, these findings indicate that the higher density of vGAT+/CB+ cartridges in schizophrenia is not attributable to either higher

CB protein levels per ChC bouton or a greater density of ChC boutons per pyramidal neuron AIS.

Interestingly, a previous study found a higher density of parvalbumin-immunoreactive cartridges in layers 5–6 of the anterior cingulate cortex (ACC) in schizophrenia (38). In addition, the same group reported that the density of parvalbumin-immunoreactive neurons is increased in layer 5 of the ACC in schizophrenia (39). Thus, in the ACC a higher density of cartridges in schizophrenia might result from a greater number of ChCs. In contrast to the ACC, the density of parvalbumin-immunoreactive neurons is unchanged in the PFC of schizophrenia subjects (40, 41), suggesting that the higher density of cartridges in PFC layer 2 in schizophrenia arise from a normal complement of ChCs.

Although the cause of higher vGAT+/CB+ cartridge density in layer 2 of schizophrenia cannot be determined by our data, the laminar specificity of the findings suggests a developmental origin. Human brain development is a highly protracted process in which some brain regions (e.g., PFC) do not reach maturity until early adulthood (42–47). In addition, within a given cortical region development generally progresses in an inside-out manner, such that layer 2 matures later relative to deeper cortical layers. In primates the number of ChC boutons per AIS declines over postnatal development, which results in a lower density of cartridges detectable by vGAT immunoreactivity (35). In addition, the density of cartridges immunoreactive for GAT1 declines with age earlier in the middle cortical layers than in layer 2 (48, 49), suggesting that the timing of ChC bouton pruning differs across layers. Thus, in schizophrenia developmental pruning of ChC boutons appears to occur normally in the middle layers, but presumably due to some later occurring event, this pruning process is arrested in layer 2. The idea of arrested development of markers of cortical neurotransmission in schizophrenia has previously been postulated based on gene expression findings (25, 50).

Such arrested development might also explain the apparent elevated levels of GABAA α2-containing receptors in AISs in the PFC of subjects with schizophrenia (19). Both the α1 and α2 subunits are found in GABAA receptors in the AIS (51, 52). In addition, in layers 2–3 of monkey PFC the expression of GABAA α1 mRNA increases and that of α2 decreases across postnatal development (53). Thus, a process of arrested development in PFC layer 2 in schizophrenia could blunt this developmental switch, resulting in higher levels of GABAA α2 protein at ChC-to-AIS synapses in schizophrenia.

Although the idea that the higher density of vGAT+/CB+ cartridges in schizophrenia results from arrested development is compelling, we cannot definitely conclude that it reflects the primary pathology of the illness. However, the higher density of vGAT+/CB+ cartridges in layer 2 in schizophrenia does not appear to be a consequence of antipsychotic exposure or illness chronicity as vGAT+/CB+ cartridge density within schizophrenia subjects did not differ as a function of the use of antipsychotics at time of death or duration of illness. In addition, a previous study that assessed cartridge density in monkeys chronically treated with antipsychotics found no evidence of drug effects (18).

In comparison subjects, CB+ cartridges were observed in layers 2–6 with the highest density in layers 5–6, which is consistent with the laminar distribution of CB+ cartridges in human temporal cortex (22). Findings from colocalization experiments in the human temporal cortex suggest that CB-containing ChCs also express parvalbumin (22). Although functional differences between CB+ and CB− ChCs are yet to be determined, the modulation of intracellular calcium dynamics in ChC boutons containing both CB and parvalbumin would presumably be different than ChC boutonss that only contained parvalbumin. With that said, both ChC bouton subtypes appear to exert their function onto PYR in the same manner, through GABA release. Thus, the higher density of layer 2 CB+ cartridges, greater levels of GABAA α2 receptors per AIS, and diminished levels of GAT1 in ChC boutons in schizophrenia suggest CB-containing ChCs make a greater contribution to inhibition-mediated network synchrony (54) in this layer in the illness. The synaptic effects of ChCs appear to be mainly inhibitory under physiological conditions (55); however, activity-dependent network fluctuations can influence the postsynaptic response in AISs such that ChC inputs are depolarizing when the network is relatively quiescent (55). Although functional imaging studies suggest that network activity in the PFC is lower in schizophrenia subjects (56) and that PFC layer 3 pyramidal neurons (57) are likely to receive less excitatory drive, the status of layer 2 pyramidal neurons in the illness has not been investigated, with the exception of the higher levels of GABAA α2 receptors in the AIS. Whether the latter finding indicates that ChC inputs to layer 2 pyramidal neurons are more hyperpolarizing or more depolarizing in schizophrenia remains difficult to infer. Given that pyramidal neurons in layers 2 and deep 3 receive afferent excitatory inputs from different sources (e.g., amygdala and thalamus, respectively), the apparent greater number and strength of ChC inputs to layer 2 pyramidal neurons in schizophrenia suggests that further mapping of the relationship between neural circuitry in layers 2 and 3 in schizophrenia is required to understand the functional status of the PFC in the illness.

Supplementary Material

Refer to Web version on PubMed Central for supplementary material.

Acknowledgments

The content is solely the responsibility of the authors and does not necessarily represent the official views of the National Institute of Mental Health, the National Institutes of Health, or the United States Government. This work was supported by the NSF (DGE-0549352 to BRR) and NIMH (MH043784 to DAL; MH096985 to KNF).

David A. Lewis currently receives investigator-initiated research support from Pfizer. In 2013–2015, he served as a consultant in the areas of target identification and validation and new compound development to Autifony, Bristol-Myers Squibb, Concert Pharmaceuticals and Sunovion.

References

1. Reichenberg A, Caspi A, Harrington H, Houts R, Keefe RS, Murray RM, et al. Static and dynamic cognitive deficits in childhood preceding adult schizophrenia: a 30-year study. Am J Psychiatry. 2010; 167:160–169. [PubMed: 20048021]
2. Akbarian S, Kim JJ, Potkin SG, Hagman JO, Tafazzoli A, Bunney WE Jr. Gene expression for glutamic acid decarboxylase is reduced without loss of neurons in prefrontal cortex of schizophrenics. Arch Gen Psychiatry. 1995; 52:258–266. [PubMed: 7702443]

3. Duncan CE, Webster MJ, Rothmond DA, Bahn S, Elashoff M, Shannon Weickert C. Prefrontal GABA(A) receptor alpha-subunit expression in normal postnatal human development and schizophrenia. J Psychiatr Res. 2010; 44:673–681. [PubMed: 20100621]
4. Guidotti A, Auta J, Davis JM, Di-Giorgi-Gerevini V, Dwivedi Y, Grayson DR, et al. Decrease in reelin and glutamic acid decarboxylase67 (GAD67) expression in schizophrenia and bipolar disorder: a postmortem brain study. Arch Gen Psychiatry. 2000; 57:1061–1069. [PubMed: 11074872]
5. Hashimoto T, Arion D, Unger T, Maldonado-Aviles JG, Morris HM, Volk DW, et al. Alterations in GABA-related transcriptome in the dorsolateral prefrontal cortex of subjects with schizophrenia. Mol Psychiatry. 2008; 13:147–161. [PubMed: 17471287]
6. Hashimoto T, Arion G, Unger T, Volk DW, Mirnics K, Lewis DA. Analysis of gaba-specific transcriptome in the prefrontal cortex of subjects with schizophrenia. Soc Neurosci Abstr. 2005:675.674.
7. Hashimoto T, Bazmi HH, Mirnics K, Wu Q, Sampson AR, Lewis DA. Conserved regional patterns of GABA-related transcript expression in the neocortex of subjects with schizophrenia. Am J Psychiatry. 2008; 165:479–489. [PubMed: 18281411]
8. Mellios N, Huang HS, Baker SP, Galdzicka M, Ginns E, Akbarian S. Molecular determinants of dysregulated GABAergic gene expression in the prefrontal cortex of subjects with schizophrenia. Biol Psychiatry. 2009; 65:1006–1014. [PubMed: 19121517]
9. Mirnics K, Middleton FA, Marquez A, Lewis DA, Levitt P. Molecular characterization of schizophrenia viewed by microarray analysis of gene expression in prefrontal cortex. Neuron. 2000; 28:53–67. [PubMed: 11086983]
10. Straub RE, Lipska BK, Egan MF, Goldberg TE, Callicott JH, Mayhew MB, et al. Allelic variation in GAD1 (GAD67) is associated with schizophrenia and influences cortical function and gene expression. Mol Psychiatry. 2007; 12:854–869. [PubMed: 17767149]
11. Vawter MP, Crook JM, Hyde TM, Kleinman JE, Weinberger DR, Becker KG, et al. Microarray analysis of gene expression in the prefrontal cortex in schizophrenia: A preliminary study. Schizophrenia Research. 2002; 58:11–20. [PubMed: 12363385]
12. Volk DW, Austin MC, Pierri JN, Sampson AR, Lewis DA. Decreased glutamic acid decarboxylase67 messenger RNA expression in a subset of prefrontal cortical gamma-aminobutyric acid neurons in subjects with schizophrenia. Arch Gen Psychiatry. 2000; 57:237–245. [PubMed: 10711910]
13. Guillozet-Bongaarts AL, Hyde TM, Dalley RA, Hawrylycz MJ, Henry A, Hof PR, et al. Altered gene expression in the dorsolateral prefrontal cortex of individuals with schizophrenia. Mol Psychiatry. 2014; 19:478–485. [PubMed: 23528911]
14. Thune JJ, Uylings HBM, Pakkenberg B. No deficit in total number of neurons in the prefrontal cortex in schizophrenics. J Psychiatr Res. 2001; 35:15–21. [PubMed: 11287052]
15. Rocco BR, Lewis DA, Fish KN. Markedly Lower Glutamic Acid Decarboxylase 67 Protein Levels in a Subset of Boutons in Schizophrenia. Biol Psychiatry. 2016; 79:1006–1015. [PubMed: 26364548]
16. Lewis DA, Lund JS. Heterogeneity of chandelier neurons in monkey neocortex: corticotropin-releasing factor- and parvalbumin-immunoreactive populations. J Comp Neurol. 1990; 293:599–615. [PubMed: 2329196]
17. Woo TU, Whitehead RE, Melchitzky DS, Lewis DA. A subclass of prefrontal gamma-aminobutyric acid axon terminals are selectively altered in schizophrenia. Proc Natl Acad Sci U S A. 1998; 95:5341–5346. [PubMed: 9560277]
18. Pierri JN, Chaudry AS, Woo TU, Lewis DA. Alterations in chandelier neuron axon terminals in the prefrontal cortex of schizophrenic subjects. Am J Psychiatry. 1999; 156:1709–1719. [PubMed: 10553733]
19. Volk DW, Pierri JN, Fritschy JM, Auh S, Sampson AR, Lewis DA. Reciprocal alterations in pre- and postsynaptic inhibitory markers at chandelier cell inputs to pyramidal neurons in schizophrenia. Cerebral Cortex. 2002; 12:1063–1070. [PubMed: 12217970]
20. Lewis DA, Hashimoto T, Volk DW. Cortical inhibitory neurons and schizophrenia. Nat Rev Neurosci. 2005; 6:312–324. [PubMed: 15803162]

21. Fung SJ, Sivagnanasundaram S, Weickert CS. Lack of change in markers of presynaptic terminal abundance alongside subtle reductions in markers of presynaptic terminal plasticity in prefrontal cortex of schizophrenia patients. Biol Psychiatry. 2011; 69:71–79. [PubMed: 21145444]
22. del Rio MR, DeFelipe J. Colocalization of parvalbumin and calbindin D-28k in neurons including chandelier cells of the human temporal neocortex. J Chem Neuroanat. 1997; 12:165–173. [PubMed: 9141648]
23. Beneyto, M., Sibille, E., Lewis, DA. Human postmortem brain research in mental illness syndromes. In: Charney, DS., Nestler, E., editors. Neurobiology of Mental Illness. New York: Oxford University Press; 2008. p. 202-214.
24. Curley AA, Arion D, Volk DW, Asafu-Adjei JK, Sampson AR, Fish KN, et al. Cortical deficits of glutamic acid decarboxylase 67 expression in schizophrenia: clinical, protein, and cell type-specific features. Am J Psychiatry. 2011; 168:921–929. [PubMed: 21632647]
25. Hoftman GD, Volk DW, Bazmi HH, Li S, Sampson AR, Lewis DA. Altered cortical expression of GABA-related genes in schizophrenia: illness progression vs developmental disturbance. Schizophr Bull. 2015; 41:180–191. [PubMed: 24361861]
26. Jiao Y, Sun Z, Lee T, Fusco FR, Kimble TD, Meade CA, et al. A simple and sensitive antigen retrieval method for free-floating and slide-mounted tissue sections. J Neurosci Meth. 1999; 93:149–162.
27. Fish KN, Sweet RA, Lewis DA. Differential distribution of proteins regulating GABA synthesis and reuptake in axon boutons of subpopulations of cortical interneurons. Cereb Cortex. 2011; 21:2450–2460. [PubMed: 21422269]
28. Rocco BR, Sweet RA, Lewis DA, Fish KN. GABA-Synthesizing Enzymes in Calbindin and Calretinin Neurons in Monkey Prefrontal Cortex. Cereb Cortex. 2016; 26:2191–2204. [PubMed: 25824535]
29. Guo C, Stella SL Jr, Hirano AA, Brecha NC. Plasmalemmal and vesicular gamma-aminobutyric acid transporter expression in the developing mouse retina. J Comp Neurol. 2009; 512:6–26. [PubMed: 18975268]
30. Gottlieb DI, Chang YC, Schwob JE. Monoclonal antibodies to glutamic acid decarboxylase. Proc Natl Acad Sci U S A. 1986; 83:8808–8812. [PubMed: 2430303]
31. Chang YC, Gottlieb DI. Characterization of the proteins purified with monoclonal antibodies to glutamic acid decarboxylase. J Neurosci. 1988; 8:2123–2130. [PubMed: 3385490]
32. Rocco BR, Sweet RA, Lewis DA, Fish KN. GABA synthesizing enzymes in calbindin and calretinin neurons in monkey prefrontal cortex. Cereb Cortex. 2015 In Press.
33. McIntire SL, Reimer RJ, Schuske K, Edwards RH, Jorgensen EM. Identification and characterization of the vesicular GABA transporter. Nature. 1997; 389:870–876. [PubMed: 9349821]
34. Chaudhry FA, Reimer RJ, Bellocchio EE, Danbolt NC, Osen KK, Edwards RH, et al. The vesicular GABA transporter, VGAT, localizes to synaptic vesicles in sets of glycinergic as well as GABAergic neurons. The Journal of Neuroscience. 1998; 18:9733–9750. [PubMed: 9822734]
35. Fish KN, Hoftman GD, Sheikh W, Kitchens M, Lewis DA. Parvalbumin-containing chandelier and basket cell boutons have distinctive modes of maturation in monkey prefrontal cortex. J Neurosci. 2013; 33:8352–8358. [PubMed: 23658174]
36. Hoaglin DC, Iglewicz B. Fine tuning some resistant rules for outlier labeling. Journal of American Statistical Association. 1987; 82:1147–1149.
37. Hoaglin DC, Iglewicz B, Tukey JW. Performance of some resistant rules for outlier labeling. Journal of American Statistical Association. 1986; 81:991–999.
38. Kalus P, Senitz D, Lauer M, Beckmann H. Inhibitory cartridge synapses in the anterior cingulate cortex of schizophrenics. J Neural Transm. 1999; 106:763–771. [PubMed: 10907735]
39. Kalus P, Senitz D, Beckmann H. Altered distribution of parvalbumin-immunoreactive local circuit neurons in the anterior cingulate cortex of schizophrenic patients. Psychiatry Res. 1997; 75:49–59. [PubMed: 9287373]
40. Hashimoto T, Volk DW, Eggan SM, Mirnics K, Pierri JN, Sun Z, et al. Gene expression deficits in a subclass of GABA neurons in the prefrontal cortex of subjects with schizophrenia. J Neurosci. 2003; 23:6315–6326. [PubMed: 12867516]

41. Enwright JF, Sanapala S, Foglio A, Berry R, Fish KN, Lewis DA. Reduced Labeling of Parvalbumin Neurons and Perineuronal Nets in the Dorsolateral Prefrontal Cortex of Subjects with Schizophrenia. Neuropsychopharmacology. 2016; 41:2206–2214. [PubMed: 26868058]
42. Michalareas G, Vezoli J, van Pelt S, Schoffelen JM, Kennedy H, Fries P. Alpha-Beta and Gamma Rhythms Subserve Feedback and Feedforward Influences among Human Visual Cortical Areas. Neuron. 2016
43. Gogtay N, Giedd JN, Lusk L, Hayashi KM, Greenstein D, Vaituzis AC, et al. Dynamic mapping of human cortical development during childhood through early adulthood. Proc Natl Acad Sci USA. 2004; 101:8174–8179. [PubMed: 15148381]
44. Johnson MH. Functional brain development in humans. Nat Rev Neurosci. 2001; 2:475–483. [PubMed: 11433372]
45. Shaw P, Kabani NJ, Lerch JP, Eckstrand K, Lenroot R, Gogtay N, et al. Neurodevelopmental trajectories of the human cerebral cortex. J Neurosci. 2008; 28:3586–3594. [PubMed: 18385317]
46. Giedd JN, Blumenthal J, Jeffries NO, Castellanos FX, Liu H, Zijdenbos A, et al. Brain development during childhood and adolescence: a longitudinal MRI study. Nat Neurosci. 1999; 2:861–863. [PubMed: 10491603]
47. Sowell ER, Peterson BS, Thompson PM, Welcome SE, Henkenius AL, Toga AW. Mapping cortical change across the human life span. Nat Neurosci. 2003; 6:309–315. [PubMed: 12548289]
48. Anderson SA, Classey JD, Conde F, Lund JS, Lewis DA. Synchronous development of pyramidal neuron dendritic spines and parvalbumin-immunoreactive chandelier neuron axon terminals in layer III of monkey prefrontal cortex. Neuroscience. 1995; 67:7–22. [PubMed: 7477911]
49. Cruz DA, Eggan SM, Lewis DA. Postnatal development of pre- and postsynaptic GABA markers at chandelier cell connections with pyramidal neurons in monkey prefrontal cortex. J Comp Neurol. 2003; 465:385–400. [PubMed: 12966563]
50. Hyde TM, Lipska BK, Ali T, Mathew SV, Law AJ, Metitiri OE, et al. Expression of GABA signaling molecules KCC2, NKCC1, and GAD1 in cortical development and schizophrenia. J Neurosci. 2011; 31:11088–11095. [PubMed: 21795557]
51. Nusser Z, Sieghart W, Benke D, Fritschy JM, Somogyi P. Differential synaptic localization of two major gamma-aminobutyric acid type A receptor alpha subunits on hippocampal pyramidal cells. Proc Natl Acad Sci U S A. 1996; 93:11939–11944. [PubMed: 8876241]
52. Kerti-Szigeti K, Nusser Z. Similar GABAA receptor subunit composition in somatic and axon initial segment synapses of hippocampal pyramidal cells. Elife. 2016; 5
53. Hashimoto T, Nguyen QL, Rotaru D, Keenan T, Arion D, Beneyto M, et al. Protracted developmental trajectories of GABAA receptor alpha1 and alpha2 subunit expression in primate prefrontal cortex. Biol Psychiatry. 2009; 65:1015–1023. [PubMed: 19249749]
54. Massi L, Lagler M, Hartwich K, Borhegyi Z, Somogyi P, Klausberger T. Temporal Dynamics of Parvalbumin-Expressing Axo-axonic and Basket Cells in the Rat Medial Prefrontal Cortex In Vivo. J Neurosci. 2012; 32:16496–16502. [PubMed: 23152631]
55. Woodruff AR, McGarry LM, Vogels TP, Inan M, Anderson SA, Yuste R. State-dependent function of neocortical chandelier cells. J Neurosci. 2011; 31:17872–17886. [PubMed: 22159102]
56. Minzenberg MJ, Laird AR, Thelen S, Carter CS, Glahn DC. Meta-analysis of 41 functional neuroimaging studies of executive function in schizophrenia. Arch Gen Psychiatry. 2009; 66:811–822. [PubMed: 19652121]
57. Glantz LA, Lewis DA. Decreased dendritic spine density on prefrontal cortical pyramidal neurons in schizophrenia. Arch Gen Psychiatry. 2000; 57:65–73. [PubMed: 10632234]

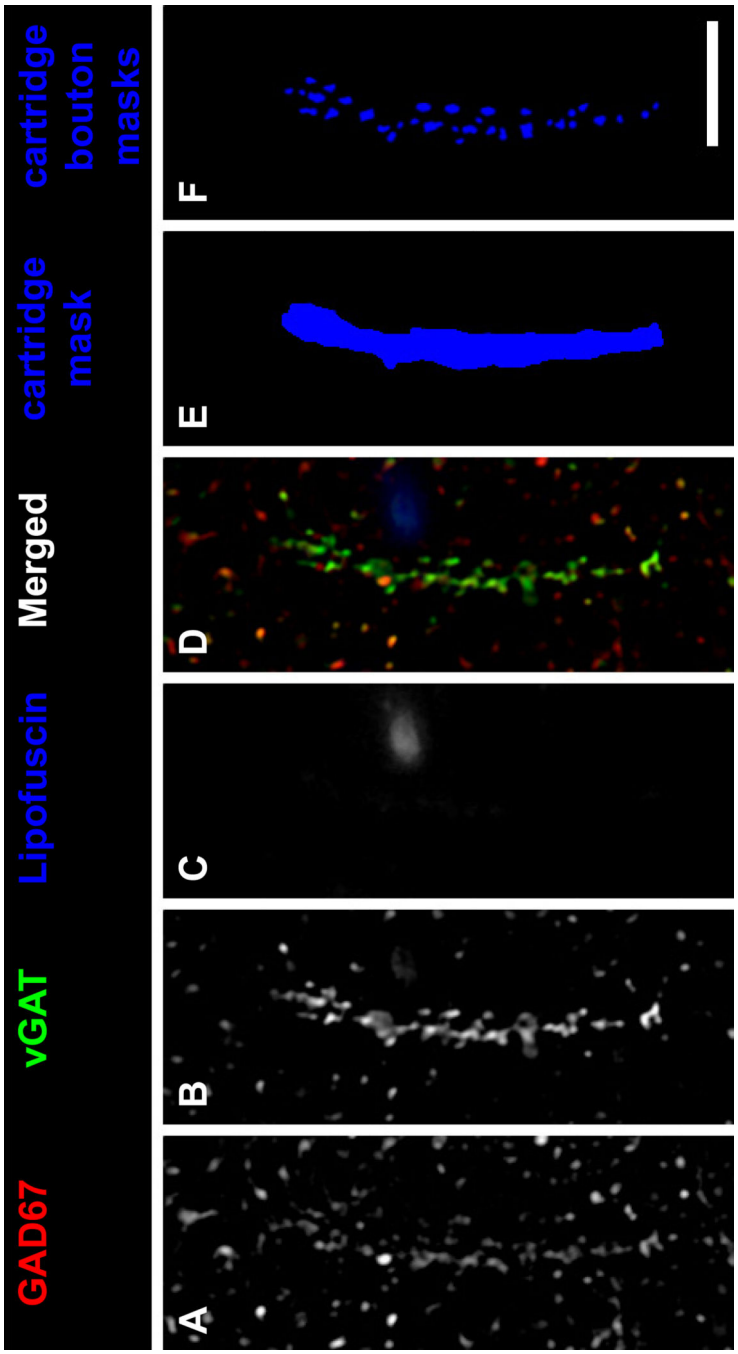

Figure 1.

ChC vGAT+ cartridge in human PFC. (A–D) A single z-plane of a human PFC tissue section immunolabeled for vGAT and GAD67. Single GAD67 (A) and vGAT (B) immunoreactive channels, and single channel of lipofuscin (C) autofluorescence. (D) Merged GAD67, vGAT, and lipofuscin channels. (E) A mask of the vGAT+ cartridge in B. (F) Individual object masks of the vGAT+ cartridge boutons that overlapped the cartridge mask in E. Bar = 10 μm.

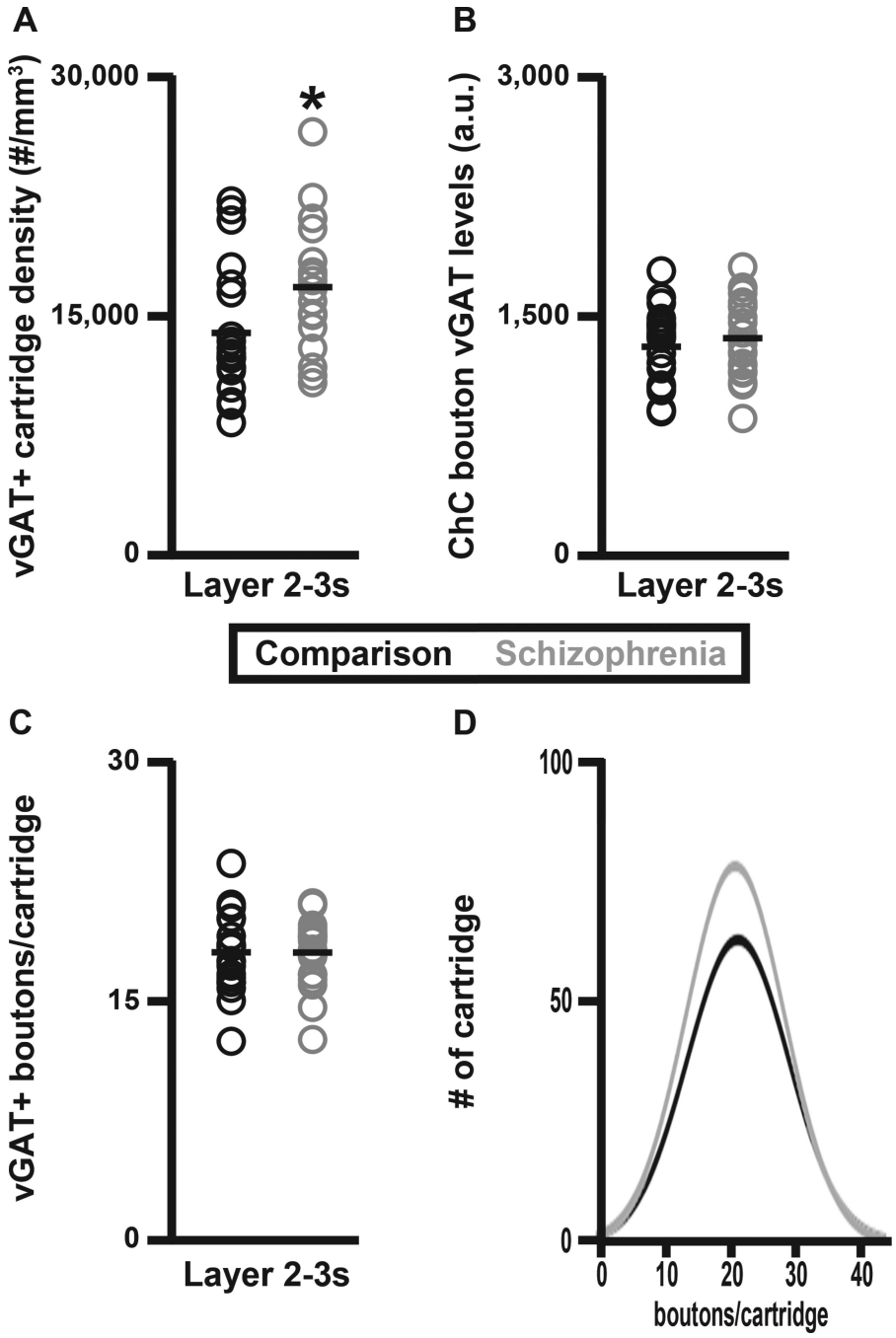

Figure 2.

vGAT+ cartridge density in PFC layer 2-superficial 3 of schizophrenia and unaffected comparison subjects. (A) The density (number/mm^3) of vGAT+ cartridges. (B) vGAT+ cartridge bouton vGAT protein levels (a.u.). (C–D) The mean number of vGAT+ boutons per vGAT+ cartridge. The asterisk in A designates a significant difference in the density of vGAT+ cartridges between schizophrenia and unaffected comparison subjects.

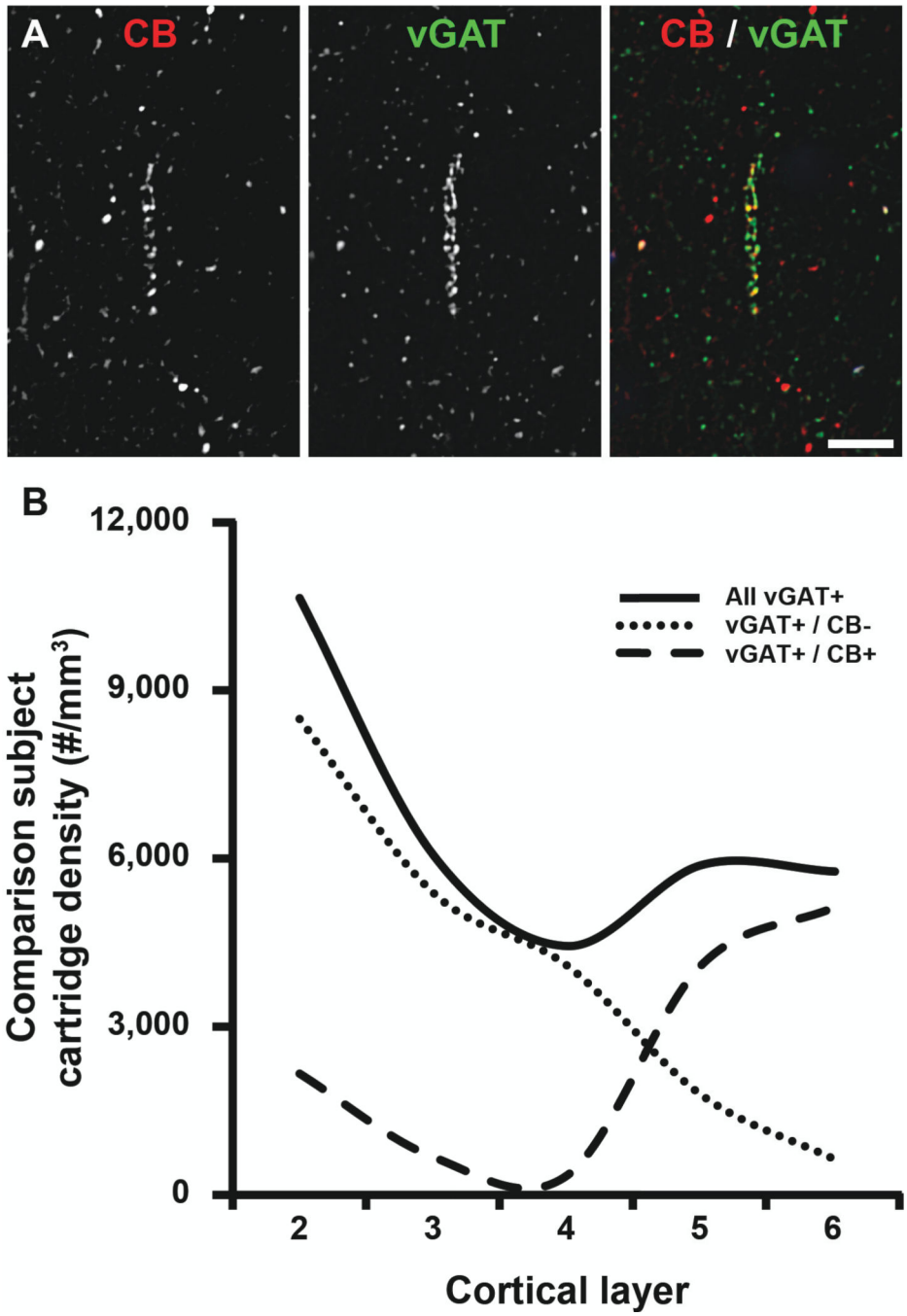

Figure 3.

ChC vGAT+/CB+ cartridges in human PFC. (A) Projection image (3 z-planes separated by 0.25 μm) of a human PFC tissue section immunolabeled for CB and vGAT. Single (CB and vGAT) and merged immunoreactive channels shown. (B) The density of all vGAT+ cartridges regardless of CB immunoreactivity (solid line), vGAT+/ CB negative cartridges (CB−; dotted line), and vGAT+/CB+ cartridges (dashed line) in cortical layers 2–6 of the human PFC.

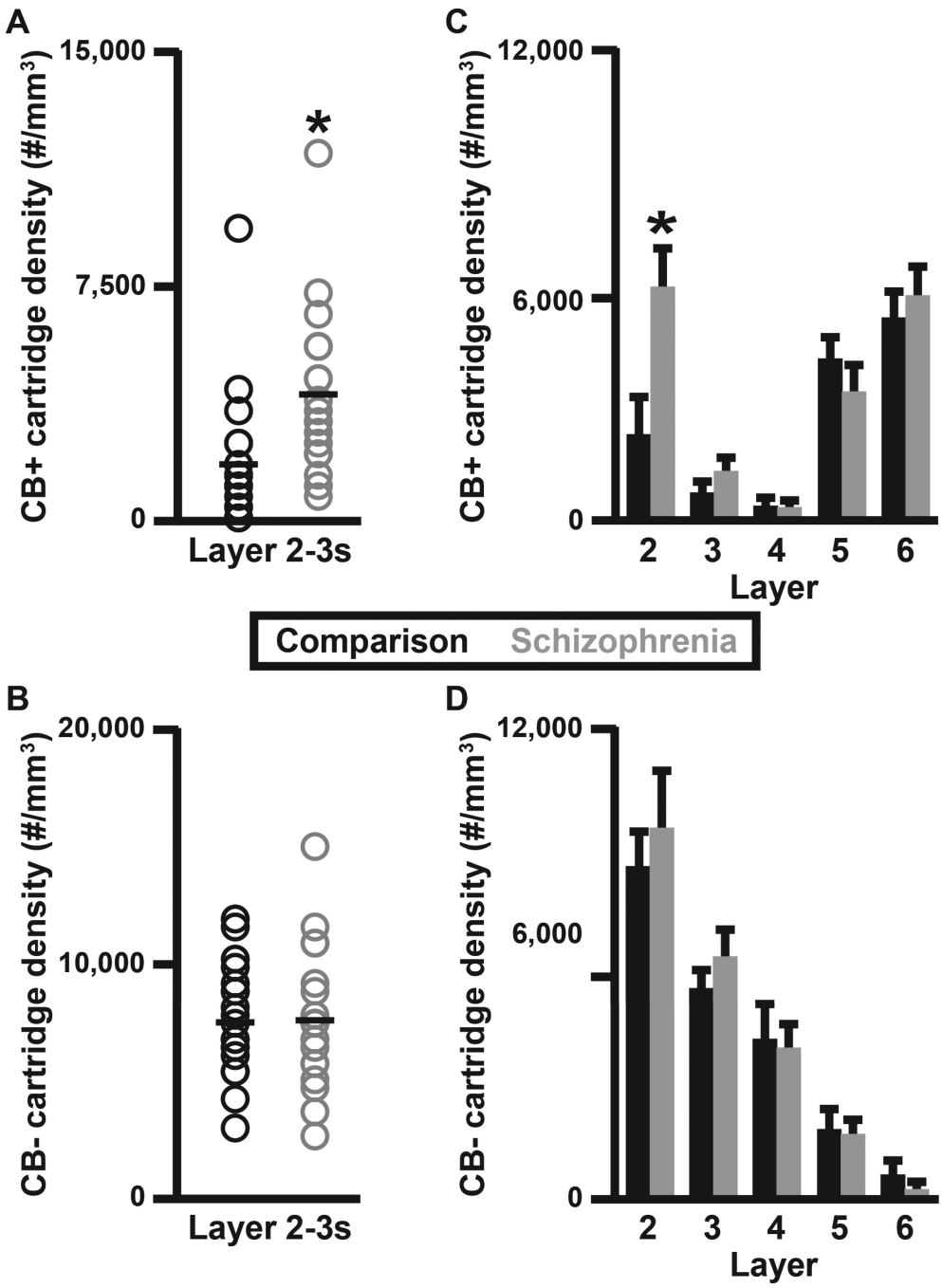

Figure 4.

Laminar analysis of ChC vGAT+/CB+ and vGAT+/CB− cartridges in schizophrenia and unaffected comparison subjects. vGAT+/CB+ (A) and vGAT+/CB− (B) cartridge density within PFC layers 2-superficial 3 (2–3s). vGAT+/CB+ (C) and vGAT+/CB− (D) cartridge density across PFC layers 2–6. The asterisks in A and C designate a significant difference in the density of vGAT+/CB+ cartridges between subject groups.

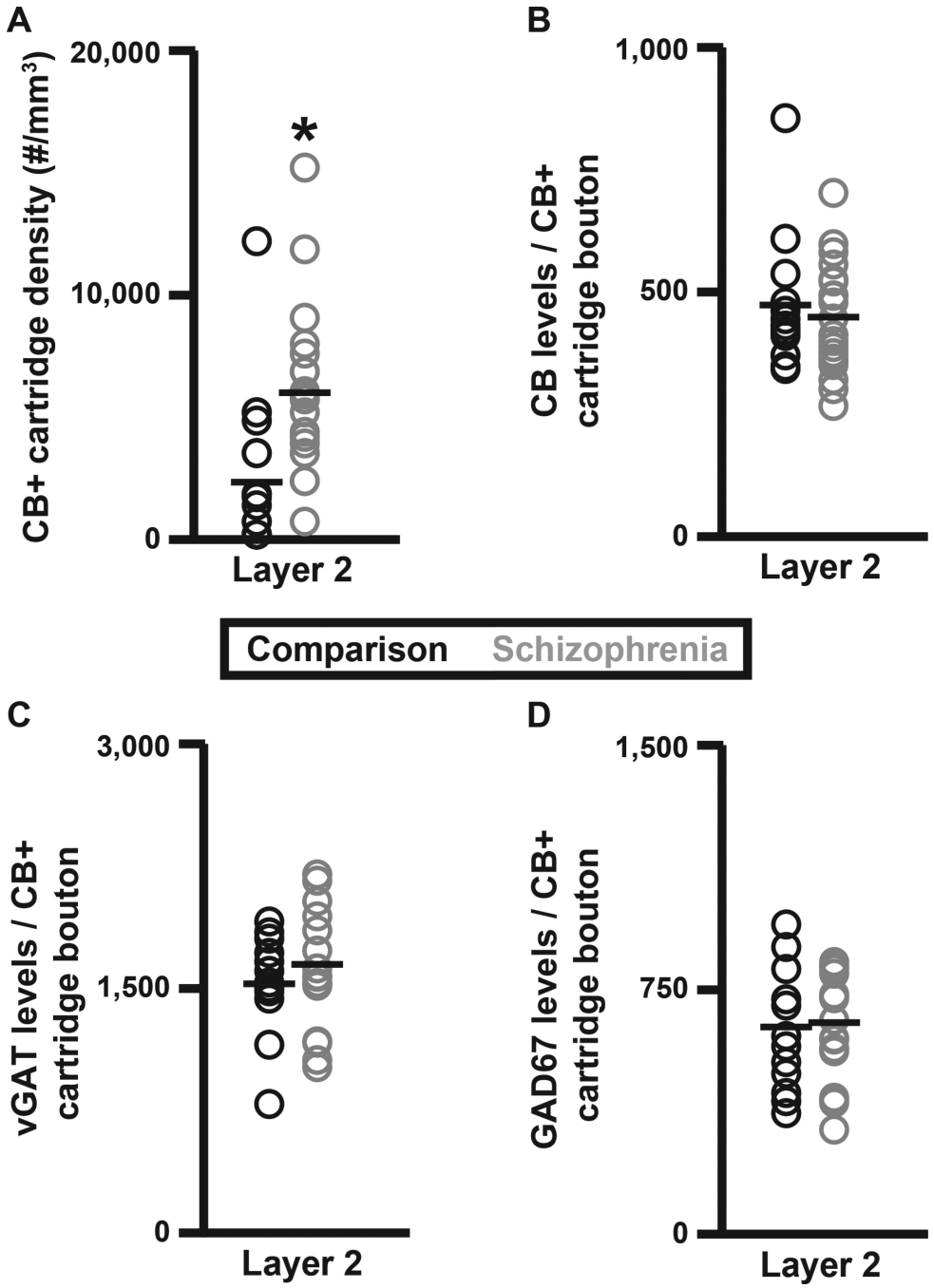

Figure 5.

Layer 2 analyses of ChC vGAT+/CB+ cartridge density and CB, vGAT, and GAD67 protein levels in schizophrenia and unaffected comparison subjects. (A) vGAT+/CB+ cartridge density. (B–D) vGAT+/CB+ cartridge bouton CB (B), vGAT (C), and GAD67 (D) protein levels (a.u.). The asterisk in A designates a significant difference in the density of vGAT +/CB+ cartridges between subject groups.

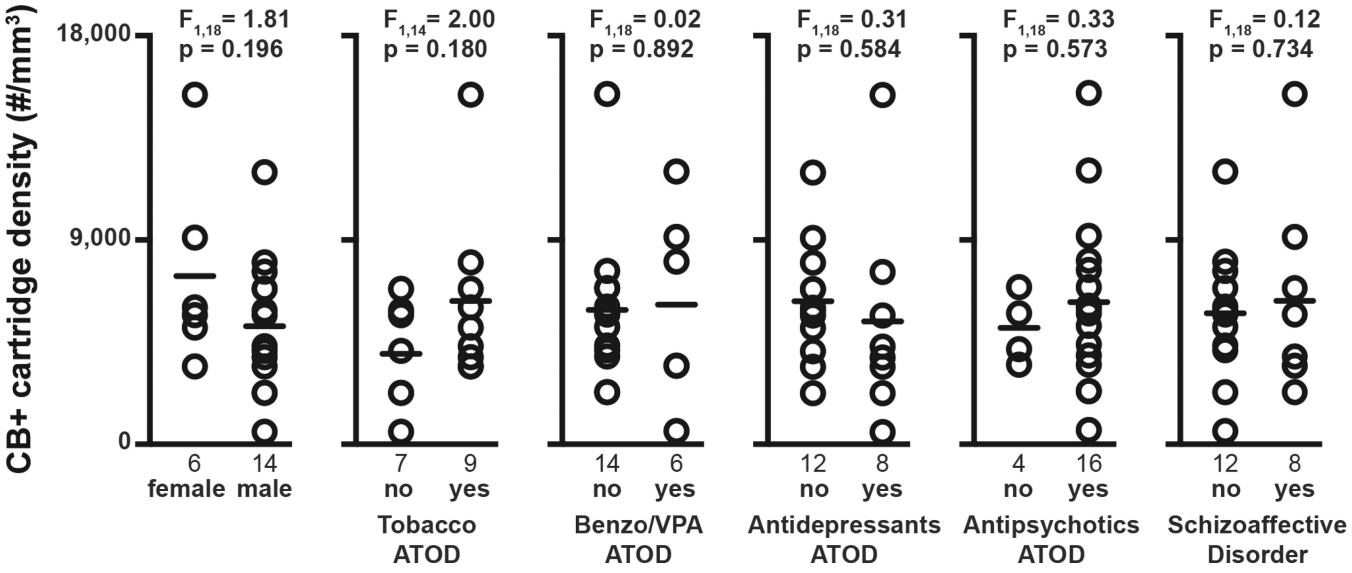

Figure 6.

Effects of comorbid factors on vGAT+/CB+ cartridge density in subjects with schizophrenia. A Bonferroni correction for multiple comparisons (n=6 dependent measures, resulting in a corrected p-value=0.008) within each comorbid factor was performed to assess their effects on vGAT+/CB+ cartridge density. ATOD, at time of death; Benzo/VPA, benzodiazepines or valproic acid.

Table 1

Summary of demographic and postmortem characteristics of human subjects. Subject groups did not differ in age ($t_{19} = 0.541$, $p = 0.545$; $t_{38} = 0.276$, $p = 0.784$), postmortem interval ($t_{19} = 0.532$, $p = 0.601$; $t_{38} = 0.327$, $p = 0.745$), or freezer storage time ($t_{19} = 0.497$, $p = 0.625$; $t_{38} = 0.268$, $p = 0.790$).

Measure	Comparison Group (N=20)	Schizophrenia Group (N=20)
Male, *n* (%)	14 (70)	14 (70)
White, *n* (%)	17 (85)	18 (90)
Black, *n* (%)	3 (15)	2 (10)
Age (years), mean ± SD	46 ± 9	45 ± 7
Postmortem interval (hours), mean ± SD	9.9 ± 4.0	9.5 ± 3.4
Tissue storage time (years), mean ± SD	14 ± 5	12 ± 5